

# The development of 6 MeV Heavy Ion Beam Probe system in LHD

A. Shimizu, T. Ido, M. Nishiura, S. Nakamura, H. Nakano, S. Ohshima<sup>1)</sup>, A. Nishizawa, M. Yokoyama, Y. Yoshimura, S. Kubo, T. Shimosuma, H. Igami, H. Takahashi, N. Tamura, I. Yamada, T. Minami, K. Narihara, T. Akiyama, T. Tokuzawa, K. Tanaka, K. Kawahata, K. Toi, M. Isobe, F. Watanabe, K. Ogawa, K. Nagaoka, K. Ikeda, M. Osakabe, K. Tsumori, Y. Takeiri, O. Kaneko, S. Kato, M. Yokota, Y. Hamada, LHD Group

*National Institute for Fusion Science, 322-6 Oroshi-cho, Toki, Gifu 509-5292, Japan*

<sup>1)</sup>*Osaka University, 2-6 Yamadaoka, Suita, Osaka 565-0871, Japan*

The 6 MeV Heavy Ion Beam Probe (HIBP) was installed to Large Helical Device (LHD) and it has been developed. The radial profile of potential in the region where normalized minor radius,  $\rho$ , is less than 0.5 was measured, and the electric field obtained from the fitting function of experimental data was compared with the neoclassical theory. The experimental results fairly coincided with the theory. The negative pulses were observed in potential signal in the case of the inward shifted magnetic configuration. The time constants of these pulses were less than the energy confinement time. Potential fluctuations of coherent modes were also observed, and one of their frequencies coincided with the geodesic acoustic mode (GAM). In this report, the present status of potential measurements with HIBP system in LHD is described.

Keywords: Large Helical Device, heavy ion beam probe, potential, tandem accelerator, tandem analyzer

## 1. Introduction

In the toroidal magnetized plasmas, radial electric field is a very important parameter. In transition phenomena, such as H-mode transition, the change of radial electric field structure was observed in tokamak [1-3]. In helical devices, the bifurcation phenomenon is predicted from the neoclassical theory, and the confinement property is improved by the produced radial electric field. In the experiment of helical device, this type of phenomenon was observed and an internal transport barrier (ITB) was created [4-6]. It is considered that the poloidal shear flow plays a very important role in the production of ITB because the shear flow can reduce the anomalous transport by suppressing the turbulence in plasma [7]. In the torus plasma, the radial electric field is related to the poloidal flow, therefore, the shear of electric field is also important. Thus, measurements of radial electric field are very essential to study these attractive physics in toroidal plasmas.

Heavy Ion Beam Probe (HIBP) [8] is a very useful tool to study these attractive physics, because it can directly measure plasma potential in the inside of high temperature toroidal plasma. Moreover, this tool can measure it with good spatial/temporal resolution, without disturbing plasma. In order to measure the radial structure of potential and its fluctuation in Large Helical Device (LHD), the 6 MeV Heavy Ion Beam Probe was installed and has been developed [9,10]. In this report,

the present status of HIBP in LHD is described and the recent results obtained from our system are shown. Up to now, the operation of this system at the acceleration energy of 6 MeV was done, however the resolution of potential measurement was not good because the acceleration voltage was not stable above  $\sim 1.3$  MV (Acceleration energy in this case corresponds to 2.6 MeV). Therefore, most data shown here were obtained on the condition of the acceleration voltage being less than 1.3 MV.

## 2. HIBP system in LHD

In Fig.1, the schematic view of HIBP system in LHD is shown. The toroidal magnetic field strength of LHD is 3 T, and the typical major/minor radius is 3.6 m / 0.6 m. In order to inject the  $\text{Au}^+$  probing beam to the center of plasma, the acceleration energy of 6 MeV is required. To reduce the required voltage to be half, the tandem accelerator is used in our system. The negative ion,  $\text{Au}^-$ , is produced in the target sputter ion source [11]. The  $\text{Au}^-$  is extracted and pre-accelerated up to 50 keV. After that, this beam is injected to the tandem accelerator and accelerated to 3 MeV. In the gas cell located in the center of the tandem accelerator,  $\text{Au}^-$  ions are stripped two electrons and changed to positive ions,  $\text{Au}^+$ . These ions are re-accelerated to 6 MeV. This beam is guided to plasma through several components: the charge separator, the 4.8 m cylindrical deflector, the 7.8 degree deflector, and so on. The orbit of probing beam has three

author's e-mail: akihiro@nifs.ac.jp

dimensional structure in the plasma. The injection angle and the ejection angle of probing beam are controlled by two 8-pole electric deflectors (sweeper) at the injection and ejection ports. By controlling these angles, the observation point is changed. The injected  $Au^+$  is stripped an electron by the collision with plasma, and at this time it obtains the potential energy at this ionized point. Here, we call the  $Au^+$  beam as the primary beam, and the produced  $Au^{2+}$  beam as the secondary beam. By measuring the difference of energy between the primary and the secondary beam, the plasma potential at the ionized point can be measured. The ionized point is called as a

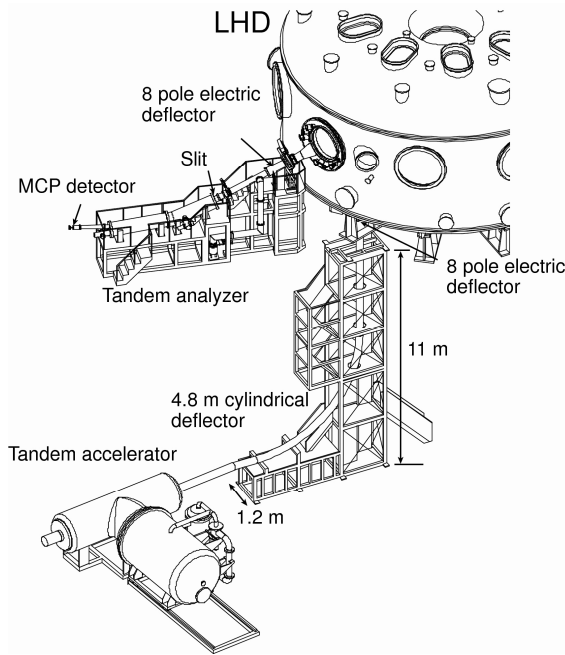


Fig.1 Schematic view of HIBP system in LHD is shown. The negative ion source is omitted in this figure.

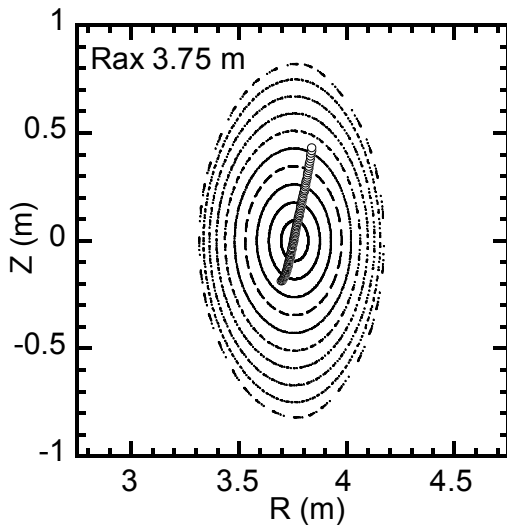


Fig.2 The projection of sample volume positions on the vertically elongated cross section and magnetic surfaces for the configuration of  $R_{ax}$  3.75 m are shown.

sample volume. The sample volume positions are arranged three dimensionally in plasma, because that the beam orbit has three dimensional geometry. The projection of sample volume positions on the vertically elongated cross section are shown in Fig.2, on the condition that the toroidal magnetic field strength is 1.5 T, the major radius of magnetic axis is 3.75 m, the acceleration energy is 1.376 MeV. The potential in the domain of the normalized minor radius from 0 to 0.5 can be measured with our HIBP system.

For the energy analyzer, if the traditional Proca-Green type of energy analyzer [12] is used, the required voltage reaches to 500 kV - 1 MV for the beam energy of 6 MeV. The electric power supply for this voltage costs much and is not realistic. Therefore the tandem type of energy analyzer is applied [13] in our system. With this analyzer, the required voltage is reduced to 120 kV with keeping the second order focusing property of the beam injection angle. There are three slit holes at the entrance of this analyzer, so

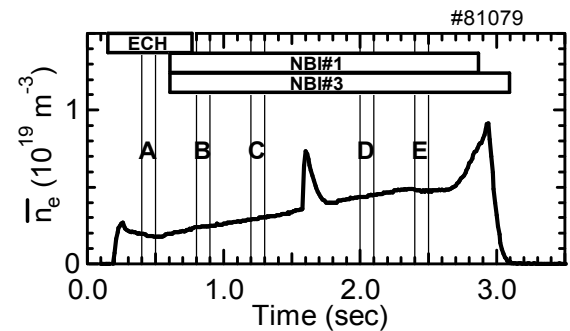


Fig.3 The temporal evolution of line averaged electron density and heating methods are shown. The potential was measured in the duration from A to E.

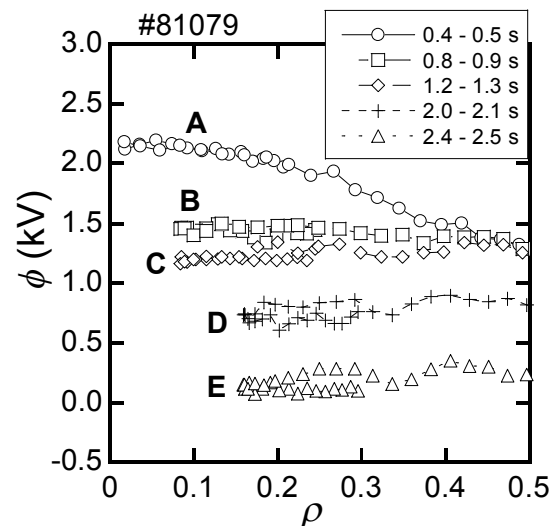


Fig.4 The radial profiles of potential measured with HIBP are shown. The characters from A to E correspond to the durations in Fig.3.

the potential of neighboring 3 sample volumes can be measured. For detecting secondary beam current, high gain detector, micro channel plates (MCPs) are used, by which a very small amount of secondary beam current can be detected. In LHD, the order of detected current is about a few tens pA - nA. The ratio of detected secondary beam current to injected primary beam current is  $10^{-5} - 10^{-4}$  in the density range of  $0.5 - 1.0 \times 10^{19} \text{ m}^{-3}$ .

### 3. The radial profile of potential

With our HIBP system, the radial profile of potential was measured. The magnetic configuration of LHD can be characterized by the major radius of the axis,  $R_{ax}$ , the toroidal magnetic field strength,  $B_t$ , the pitch parameter,  $\gamma$ , and the quadrupole component of magnetic field,  $B_q$ . The radial potential profile was measured in the magnetic field configuration of a standard one,  $R_{ax} = 3.75 \text{ m}$ ,  $B_t = 1.5 \text{ T}$ ,

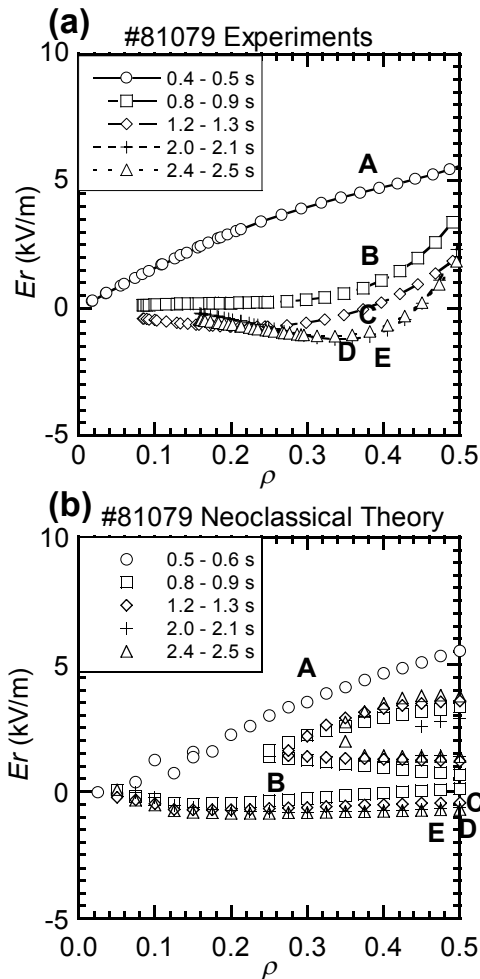


Fig.5 (a) Radial profiles of radial electric field obtained from the derivatives of the fitting functions of experimental data are shown. (b) Radial profiles of radial electric field calculated from the neoclassical theory are shown.

$\gamma = 1.254$ ,  $B_q = 100 \%$ . The energy of probing beam was 1.376 MeV. The plasma was produced by ECH and sustained by NBI heating. The line averaged density was about  $0.2 \times 10^{19} \text{ m}^{-3}$  at ECH phase, and it gradually increased. Fig.3 shows the temporal evolution of line averaged density and the heating methods. Central temperature was about 2.5 keV in ECH phase and 1.0 keV in NBI phase. The position of sample volume was changed by changing the injection angle of probing beam at 10 Hz. The radial profiles of potential obtained from HIBP in the duration from A to E are shown in Fig.4. In ECH phase, the potential was positive at the center, and it gradually decreased as the density increased. In the NBI phase, the potential at the central region was positive however the electric field was almost zero or a little negative.

By fitting these experimental data with polynomial functions and differentiating them, the profiles of electric field were obtained and compared with the neoclassical theory as shown in Fig.5. Fig.5 (a) shows the radial profile of electric field obtained from the fitting function of experimental results and Fig.5 (b) shows the calculation results estimated from the neoclassical theory. In Fig.5 (b), in the region where  $\rho > 0.25$ , the multiple roots exist. In this region, the largest positive one corresponds to the electron root, and the smallest negative one or almost zero corresponds to the ion root. The one between these roots is the unstable root. The theoretical calculations are

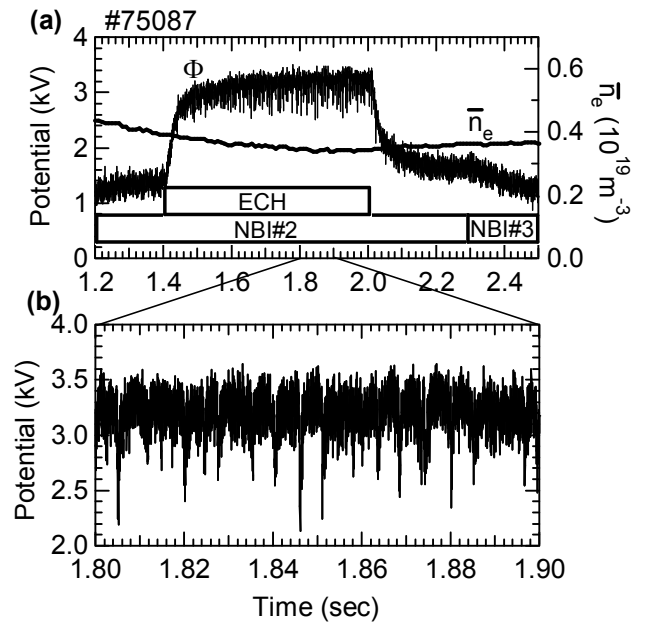


Fig.6 (a) Temporal evolutions of potential, line averaged density, heating methods are shown. (b) The magnification of potential signal from 1.8 to 1.9 sec is shown.

almost consistent with experimental results, so we can conclude that the electric field in the core region of this experiment is almost determined by the neoclassical theory.

### 3. Negative pulses observed in potential signal

In the case of the inward shifted configuration, the negative pulses were observed in the potential signal. The parameters for this magnetic configuration were as follows:  $R_{ax} = 3.6$  m,  $B_t = 1.5$  T,  $\gamma = 1.254$ ,  $B_q = 100\%$ . In this case, the probing beam energy of HIBP was 1.562 MeV. Plasma was produced by co-injection NB heating and sustained by it. Temporal evolutions of heating methods, line averaged density, and potential are shown in Fig.6 (a). The line averaged density is about  $0.4 \times 10^{19}$  m<sup>-3</sup>. At the 1.4 sec, the ECH was additionally applied. In the ECH phase, negative pulses were observed as shown in Fig.6 (b). The normalized minor radius of the sample volume position was fixed at  $\sim 0.3$ . Negative pulses can be seen in the temporal evolution of potential signal. The typical time constants are 90  $\mu$ s in the drop phase and 500  $\mu$ s in the recovering phase as shown in Fig.7. The energy confinement time is  $\sim 100$  ms in LHD. The time constant of negative pulses were much faster than the energy confinement time, so these phenomena are considered to be the bifurcation of the electric field.

In CHS, such bifurcation phenomena were observed [14,15], which is called as "pulsation". In CHS, various types of pulsation were observed. In the case of low density, the drop of potential was very large. The potential at the center in the additional ECH phase was  $\sim 1$  keV in the electron root, and it dropped to a few hundreds eV in the ion root. The change of potential was  $\sim 1$  keV. However, in the high density case in CHS, the drop of potential was small: the change of potential was about 100  $\sim 200$  eV. The result of LHD is very similar to the high

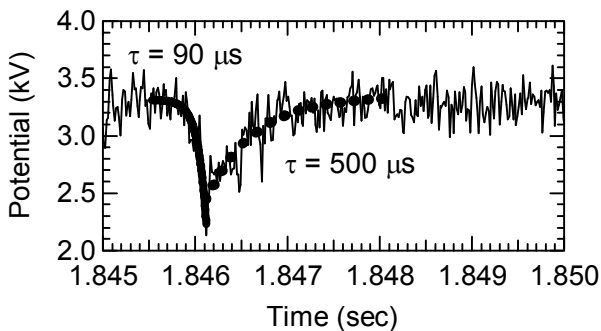


Fig.7 The time constants of negative pulse are shown. These were faster than the energy confinement time.

density case of CHS. These negative pulses were observed only the inward shift case,  $R_{ax} = 3.6$  m, and were not observed in the other configuration at present. The reason for it may be the difference of configuration property in the context of neoclassical theory.

### 4. Observation of coherent modes

The signal to noise ratio of our system was improved, so coherent modes were observed in LHD. An example of it is shown in Fig.8. As shown in Fig.8 (a), the plasma was produced and sustained by NB heating. The line averaged density was about  $0.1 \times 10^{19}$  m<sup>-3</sup>, relatively low. The ECH was applied from 1.0 to 1.6 sec, which was injected for co-directed current drive. In Fig.8 (b), the spectrogram of potential signal are shown. The position of sample volume was  $\rho \sim 0$ . These signals had the coherence with signals of magnetic probes, therefore these are considered to be the coherent modes caused by MHD instabilities. In this case, the rotational transform at the central region was increased by ECH current drive, and the shear in the rotational transform profile in the central regime becomes small. Then, it is considered that a sort of Alfvén Eigen modes were excited. Around the frequency of 20 kHz from 1.68 to 1.76 sec, the fluctuation having constant frequency was seen, which coincided with the geodesic acoustic mode (GAM) [16,17]. This mode

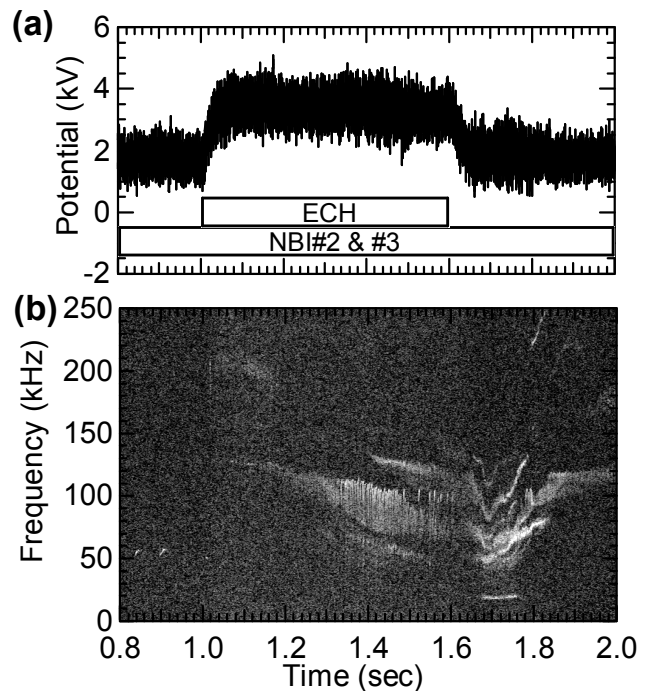


Fig.8 (a) The temporal evolution of potential and heating methods are shown. (b) The spectrogram of potential fluctuation is shown.

was localized to the central region of plasma [18]. The fluctuation amplitude was several hundreds volts.

Up to now, the fluctuation caused by turbulence was not measured clearly in the potential signal, because the signal to noise ratio of our system was not sufficient. The more improvement of S/N ratio is needed in the future.

## 5. Summary

In LHD, 6 MeV Heavy Ion Beam Probe has been developed. On the condition of the acceleration energy begin below 2.6 MeV, the acceleration energy was stable, so the potential in plasma could be measured with a good signal to noise ratio. The radial potential profile was measured in the magnetic field configuration  $R_{ax} = 3.75$  of LHD. Results were compared with the neoclassical theory. The radial profile of electric field obtained from the experiment fairly coincides with the theoretical calculation. In the inward shifted configuration ( $R_{ax} = 3.6$ ), the negative pulses were observed in potential signal. The fluctuations of coherent modes were measured with HIBP. The frequency of one of them coincided with the GAM. The fluctuation amplitudes were about several hundreds volts.

## Acknowledgments

This work was supported by the NIFS budget under contract No. ULBB 505, 514, 515, and was partly supported by MEXT Japan under Grant-in-Aid for Young Scientists (Nos. 16760674, 18760640), and NIFS/NINS under the project of Formation of International Network for Scientific Collaborations. The authors wish to thank for continuous support of scientific and technical staff in LHD.

## References

- [1] K. Ida, S. Hidekuma, Y. Miura, T. Fujita, M. Mori, K. Hoshino, N. Suzuki, T. Yamauchi *et al.*, Phys. Rev. Lett. **65**, 1364 (1990).
- [2] R. J. Groebner, K. H. Burrell, R. P. Seraydarian *et al.*, Phys. Rev. Lett. **64**, 3015 (1990).
- [3] T. Ido, K. Kamiya, Y. Miura, Y. Hamada, A. Nishizawa, Y. Kawasumi, Phys. Rev. Lett. **88**, 055006 (2002).
- [4] A. Fujisawa, H. Iguchi, T. Minami, Y. Yoshimura, H. Sanuki, K. Itoh, S. Lee, K. Tanaka *et al.*, Phys. Rev. Lett. **82**, 2669 (1999).
- [5] A. Fujisawa, H. Iguchi, T. Minami, Y. Yoshimura, K. Tanaka, K. Itoh, H. Sanuki, S. Lee, M. Kojima, S. -I. Itoh, M. Yokoyama, S. Kado, S. Okamura, R. Akiyama, K. Ida *et al.*, Phys. Plasmas **7**, 4152 (2000).
- [6] T. Estrada, A. Alonso, A. A. Chmyga, N. Dreval, L. Eliseev, C. Hidalgo, A. D. Komarov, A. S. Kozachok *et al.*, Plasma Phys. Control. Fusion **47**, L57 (2005).
- [7] K. H. Burrell, Phys. Plasmas **4**, 1499 (1997).
- [8] T. P. Crowley *et al.*, IEEE Trans. on Plasma Sci. **22**, 291 (1994).
- [9] T. Ido, A. Shimizu, M. Nishiura, A. Nishizawa, S. Katoh, K. Tsukada, M. Yokota, H. Ogawa, T. Inoue, Y. Hamada *et al.*, Rev. Sci. Instrum. **77**, 10F523 (2006).
- [10] A. Shimizu, T. Ido, M. Nishiura, H. Nakano, I. Yamada, K. Narihara, T. Akiyama, T. Tokuzawa, K. Tanaka *et al.*, J. Plasma Fusion Res. **2**, S1098 (2007).
- [11] M. Nishiura, T. Ido, A. Shimizu, S. Kato, K. Tsukada, A. Nishizawa, Y. Hamada, Y. Matsumoto *et al.*, Rev. Sci. Instrum. **77**, 03A537 (2006).
- [12] G. A. Proca and T. S. Green, Rev. Sci. Instrum. **41**, 1778 (1970).
- [13] Y. Hamada, A. Fujisawa, H. Iguchi, A. Nishizawa, Y. Kawasumi, Rev. Sci. Instrum. **68**, 2020 (1997).
- [14] A. Fujisawa, H. Iguchi, H. Idei, S. Kubo, K. Matsuoka, S. Okamura, K. Tanaka, T. Minami, S. Ohdachi, S. Morita, H. Zushi *et al.*, Phys. Rev. Lett. **81**, 2256 (1998).
- [15] A. Fujisawa, H. Iguchi, T. Minami, Y. Yoshimura, K. Tanaka, K. Itoh, H. Sanuki, S. Lee, M. Kojima, S. -I. Itoh *et al.*, Phys. Plasmas **7**, 4152 (2000).
- [16] N. Winsor, J. L. Johnson, J. M. Dowson, Phys. Fluids **11**, 2448 (1968).
- [17] P. H. Diamond, S. -I. Itoh, K. Itoh, T. S. Hahm, Plasma Phys. Control. Fusion **47**, R35 (2005).
- [18] T. Ido, A. Shimizu, M. Nishiura, H. Nakano, S. Ohshima, S. Kato, Y. Hamada, Y. Yoshimura, S. Kubo, T. Shimozuma, H. Igami, H. Takahashi, K. Toi *et al.*, Rev. Sci. Instrum. **79**, 10F318 (2008).